Available online at www.sciencedirect.com
SCIENCE DIRECT®
Journal of Solid State Chemistry 177 (2004) 1919–1924
JOURNAL OF SOLID STATE CHEMISTRY
http://elsevier.com/locate/jssc

$Yb_3Cu_6Sn_5$, $Yb_5Cu_{11}Sn_8$ and $Yb_3Cu_8Sn_4$: crystal structure of three ordered compounds

M.L. Fornasini,[a,*] P. Manfrinetti,[b] D. Mazzone,[c] P. Riani,[c] and G. Zanicchi[c]

[a] *Sezione di Chimica Fisica, Dipartimento di Chimica e Chim. Ind., Università di Genova, Via Dodecaneso 31, 16146 Genova, Italy*
[b] *INFM and Sezione di Chimica Fisica, Dipartimento di Chimica e Chim. Ind., Università di Genova, Via Dodecaneso 31, 16146 Genova, Italy*
[c] *INSTM and Sezione di Chimica Inorganica, Dipartimento di Chimica e Chim. Ind., Università di Genova, Via Dodecaneso 31, 16146 Genova, Italy*

Received 31 October 2003; received in revised form 22 January 2004; accepted 1 February 2004

Abstract

$Yb_3Cu_6Sn_5$, $Yb_5Cu_{11}Sn_8$ and $Yb_3Cu_8Sn_4$ compounds were prepared in sealed Ta crucibles by induction melting and subsequent annealing. The crystal structures of $Yb_3Cu_6Sn_5$ and $Yb_5Cu_{11}Sn_8$ were determined from single crystal diffractometer data: $Yb_3Cu_6Sn_5$, isotypic with $Dy_3Co_6Sn_5$, orthorhombic, *Immm*, *oI*28, $a = 4.365(1)$ Å, $b = 9.834(3)$ Å, $c = 12.827(3)$ Å, $Z = 2$, $R = 0.019$, 490 independent reflections, 28 parameters; $Yb_5Cu_{11}Sn_8$ with its own structure, orthorhombic, *Pmmn*, *oP*48, $a = 4.4267(6)$ Å, $b = 22.657(8)$ Å, $c = 9.321(4)$ Å, $Z = 2$, $R = 0.047$, 1553 independent reflections, 78 parameters. Both compounds belong to the $BaAl_4$-derived defective structures, and are closely related to $Ce_3Pd_6Sb_5$ (*oP*28, *Pmmn*). The crystal structure of $Yb_3Cu_8Sn_4$, isotypic with $Nd_3Co_8Sn_4$, was refined from powder data by the Rietveld method: hexagonal, $P6_3mc$, *hP*30, $a = 9.080(1)$ Å, $c = 7.685(1)$ Å, $Z = 2$, $R_{wp} = 0.040$. It is an ordered substitution derivative of the $BaLi_4$ type (*hP*30, $P6_3/mmc$). All compounds show strong Cu–Sn bonds with a length reaching 2.553(3) Å in $Yb_5Cu_{11}Sn_8$.
© 2004 Elsevier Inc. All rights reserved.

Keywords: Intermetallics; Crystal structure; Ytterbium; Copper; Tin

1. Introduction

The rare earth copper stannides have been widely investigated owing to their interesting magnetic and transport properties. In the last few years systematic studies on ternary phase diagrams and crystal structures have been performed for the light and heavy rare earths and for Y [1–8], in order to acquire a better knowledge of the ternary phases existing and of their behavior.

The isothermal section at 400°C of the Yb–Cu–Sn phase diagram showed a large number of ternary compounds [5], among which only $\tau_7 Yb_5CuSn_3$ (*hP*18, Hf_5CuSn_3-type) had previously been studied. The two $\tau_1 YbCu_{4.4}Sn_{0.6}$ (*cF*24, $MgCu_4Sn$-type) and τ_2 "$Yb_3Cu_{13}Sn_4$" (related to *hP*28 $CeNi_5Sn$) ternary phases presented an homogeneity field with an increasing Sn content, and their crystal structures were determined by single crystal and powder data, respectively. All other compounds presented a nearly stoichiometric composition. The crystal structures have been determined by powder or single crystal diffractometry for τ_4 $YbCu_9Sn_4$ (*cF*112, $NaZn_{13}$-type), τ_6 YbCuSn (*oI*12, $CeCu_2$-type) and τ_9 $Yb_3Cu_4Sn_4$ (*oI*22, $Gd_6Cu_8Ge_8$-type), while the structures of τ_3 $Yb_{14}Cu_{60}Sn_{26}$, $\tau_5 \sim Yb_{30}Cu_{39}Sn_{31}$, τ_8 $Yb_{23}Cu_{42}Sn_{35}$ and τ_{10} $Yb_{36}Cu_{18}Sn_{46}$ remained unsolved. Afterwards the τ_{10} $Yb_{36}Cu_{18}Sn_{46}$ phase has been found to crystallize in a new structure type with formula $Yb_4Cu_2Sn_5$ (*oP*22) [8].

Pursuing the structural determination of the other phases, some test alloys were examined in a restricted region of the diagram, ranging from 20 to 27 at% ytterbium and 27–36 at% tin. Besides the τ_8 $Yb_{23}Cu_{42}Sn_{35}$ phase, two new ternary compounds were identified. This work reports on the crystal structure of these three phases, namely $Yb_3Cu_6Sn_5$, $Yb_5Cu_{11}Sn_8$ and $Yb_3Cu_8Sn_4$.

2. Experimental

The metals used were ytterbium, copper and tin of 99.9, 99.99 and 99.999 wt% purity, respectively. To avoid any weight losses due to possible volatilization of

*Corresponding author. Fax: +39-010-3628252.
E-mail address: cfmet@chimica.unige.it (M.L. Fornasini).

0022-4596/$ - see front matter © 2004 Elsevier Inc. All rights reserved.
doi:10.1016/j.jssc.2004.02.007

ytterbium, the alloys were prepared in sealed Ta crucibles. Stoichiometric amounts of the constituent metals in form of turnings (total mass of about 2–3 g) were pressed together directly into outgassed tantalum crucibles which were sealed by arc welding under a flow of pure argon. The samples were melted by slowly heating the crucibles in a high-frequency induction furnace up to the liquid state and shaken to ensure homogeneization. To determine the liquidus and most of the characteristic temperatures, specimens prepared as above and closed by arc welding into Mo crucibles, were transferred to a differential thermal analysis equipment (DTA) and subjected to heating and cooling cycles at rates of 5 or 10°C/min; the temperature measurements were accurate to within ±5°C. No contamination of the alloys due to reactivity towards the container material (Ta, Mo) was noticeable, even when much higher temperatures than the liquidus were reached. The $Yb_3Cu_8Sn_4$ and $Yb_{20.4}Cu_{46.5}Sn_{33.1}$ samples were annealed at 640°C for 34 days and at 620°C for 7 days, respectively.

For the metallographic examination, both optical and electron microscopy (SEM) were employed, while electron probe microanalysis (EPMA) of the phases was performed using the Oxford spectrometer INCA Energy 300.

X-ray analysis was carried out by both powder and single crystal methods. Powder patterns were obtained by a Guinier-Stoe camera using the Cu$K\alpha$ radiation and pure Si as an internal standard ($a = 5.4308$ Å); the Guinier patterns were indexed with the aid of the LAZY-PULVERIX program [9] and the lattice parameters determined by least-squares methods. Single crystal intensities of $Yb_3Cu_6Sn_5$ and $Yb_5Cu_{11}Sn_8$ were collected at 293 K on a MACH3 (Bruker-Nonius) diffractometer with graphite-monochromated Mo$K\alpha$ radiation ($\lambda = 0.7107$ Å) and lattice parameters obtained from 25 diffractometer-measured reflections at $\theta = 24°$–$28°$. Absorption correction was applied using ψ-scans of three top reflections for both crystals. Powder data of the $Yb_3Cu_8Sn_4$ compound were collected on a Philips PW1050/81 diffractometer with Bragg-Brentano geometry with Ni-filtered Cu$K\alpha$ radiation ($\lambda = 1.5418$ Å), in 2θ steps of 0.02° and a measuring time of 18 s/step. A total number of 119 reflections and 4000 profile points were processed, using pseudo-Voigt functions for peak shape and a 5th order polynomial for the background.

3. Results

A single crystal of the phase $Yb_3Cu_6Sn_5$ was picked out in a DTA sample with composition $Yb_{27}Cu_{37}Sn_{36}$ slowly cooled at 5°C/min and preliminary data gave strong evidence of its isotypism with the $Dy_3Co_6Sn_5$ structure [10], ordered ternary variant of the La_3Al_{11} type [11]. For the $Yb_5Cu_{11}Sn_8$ compound the search for single crystals was made in a sample with composition $Yb_{20.4}Cu_{46.5}Sn_{33.1}$, prepared following the microprobe analysis results. The structure was solved with the SIR97 program [12] in the centrosymmetric space group *Pmmn*, according to the systematic extinctions and statistical tests on the center of symmetry. Least-squares refinements based on F_o^2 were made by SHELXL-97 [13] for both structures, using anisotropic displacement parameters and weights $w = 1/[\sigma^2(F_o^2) + (aP)^2 + bP]$. The crystal data are reported in Table 1, while atomic coordinates standardized with STRUCTURE TIDY [14] and equivalent isotropic displacement parameters are given in Tables 2 and 3 for $Yb_3Cu_6Sn_5$ and $Yb_5Cu_{11}Sn_8$, respectively. The lattice parameters obtained from Guinier powder patterns of the two phases ($Yb_3Cu_6Sn_5$: $a = 4.370(3)$ Å, $b = 9.847(6)$ Å, $c = 12.833(6)$ Å; $Yb_5Cu_{11}Sn_8$: $a = 4.426(1)$ Å, $b = 22.648(5)$ Å, $c = 9.319(3)$ Å) are in good agreement with the single crystal values.

Further details of the crystal structure investigations can be obtained from the Fachinformationszentrum Karlsruhe, 76344 Eggenstein-Leopoldshafen, Germany, (fax (49)7247-808-666; e-mail: crysdata@fiz.karlsruhe.de) on quoting the depository number CSD-413485 ($Yb_3Cu_6Sn_5$) and CSD-413486 ($Yb_5Cu_{11}Sn_8$).

Holes in the atomic arrangement of $Yb_3Cu_6Sn_5$ and $Yb_5Cu_{11}Sn_8$ were searched for by the program CAVITY [15]. In both structures the largest holes are tetrahedral, delimited by 2Yb + 2Sn atoms at 0, 0.62, 1/2 with a radius of 0.54 Å and 1/4, 3/4, 0.86 with a radius of 0.62 Å, respectively. These values are in the normal range for intermetallic compounds.

For the third phase studied in this work, $Yb_3Cu_8Sn_4$, owing to the small size of the crystallites, no suitable crystal could be isolated. However, its Guinier powder pattern could be easily indexed on the basis of the hexagonal $Nd_3Co_8Sn_4$ structure [16] and the lattice constants values $a = 9.080(1)$ Å, $c = 7.685(1)$ Å were derived. The atomic parameters of the isotypic $Eu_3Cu_8Sn_4$ phase, determined by single crystal [17], were used as the starting point for a refinement by the Rietveld method [18]. Since the data also showed very few reflections of another hexagonal phase of the Yb–Cu–Sn system, related to the $CeNi_5Sn$ structure [5], the two compounds were refined together. The lattice parameters of $Yb_3Cu_8Sn_4$ obtained after refining, $a = 9.079(1)$ Å, $c = 7.685(1)$ Å are in excellent agreement with the Guinier pattern data. The results are given in Table 4; the observed and calculated X-ray patterns together with the difference between observed and calculated data are shown in Fig. 1.

The interatomic distances for $Yb_3Cu_6Sn_5$ and $Yb_5Cu_{11}Sn_8$ are listed in Tables 5 and 6.

Table 1
Crystal data of $Yb_3Cu_6Sn_5$ and $Yb_5Cu_{11}Sn_8$

	$Yb_3Cu_6Sn_5$	$Yb_5Cu_{11}Sn_8$
Pearson code	*oI*28	*oP*48
Space group, Z	*Immm* (No. 71), 2	*Pmmn* (No. 59), 2
Lattice parameters (Å)	$a = 4.365(1)$	$a = 4.4267(6)$
	$b = 9.834(3)$	$b = 22.657(8)$
	$c = 12.827(3)$	$c = 9.321(4)$
Cell volume (Å^3), Formula weight	550.6(3), 1494	934.9(5), 2514
Calculated density (mg/m^3)	9.01	8.93
Crystal size (mm^3)	$0.05 \times 0.05 \times 0.08$	$0.02 \times 0.06 \times 0.09$
Scan mode, θ range (deg)	$\omega - \theta$; 2–30	$\omega - \theta$; 2–30
Range in h, k, l	0 +6; ±13; ±18	0 +6; ±31; 0 +13
Reflections collected/unique	1786/490 [$R_{int} = 0.059$]	3201/1553 [$R_{int} = 0.043$]
Absorption coefficient (mm^{-1})	47.6	47.4
Transmission ratio (max/min)	1.92	1.97
Reflections with $F_o > 4\sigma(F_o)$	413	1058
Number of parameters	28	78
Extinction coefficient	0.0055(2)	0.00070(7)
a, b values in weight formula	0.0231,0.0	0.0685,0.0
w$R(F_o^2)$, all data	0.046	0.109
$R[F_o > 4\sigma(F_o)]$	0.019	0.047
Goodness of fit (S)	1.043	0.946
$\Delta\rho_{min}$, $\Delta\rho_{max}$ (e Å^{-3})	−2.0, 1.8	−5.9, 5.6

Table 2
Atomic coordinates and equivalent isotropic displacement parameters for $Yb_3Cu_6Sn_5$

Atom	Position	*x*	*y*	*z*	U_{eq} (Å^2)
Yb1	4*i*	0	0	0.30821(4)	0.0096(2)
Yb2	2*a*	0	0	0	0.0128(2)
Cu1	8*l*	0	0.2832(1)	0.1217(1)	0.0137(3)
Cu2	4*h*	0	0.1930(2)	1/2	0.0136(3)
Sn1	8*l*	0	0.34743(6)	0.33069(4)	0.0105(2)
Sn2	2*d*	1/2	0	1/2	0.0102(3)

Table 3
Atomic coordinates and equivalent isotropic displacement parameters for $Yb_5Cu_{11}Sn_8$. Origin at center

Atom	Position	*x*	*y*	*z*	U_{eq} (Å^2)
Yb1	4*e*	1/4	0.03853(4)	0.7425(1)	0.0090(2)
Yb2	4*e*	1/4	0.65556(4)	0.7093(1)	0.0120(2)
Yb3	2*a*	1/4	1/4	0.7631(1)	0.0097(3)
Cu1	4*e*	1/4	0.0314(1)	0.0824(3)	0.0136(6)
Cu2	4*e*	1/4	0.1399(1)	0.0251(4)	0.0223(7)
Cu3	4*e*	1/4	0.1442(1)	0.5357(3)	0.0143(6)
Cu4	4*e*	1/4	0.5568(1)	0.4866(3)	0.0136(6)
Cu5	4*e*	1/4	0.6959(1)	0.0261(3)	0.0131(6)
Cu6	2*b*	1/4	3/4	0.4564(5)	0.0225(9)
Sn1	4*e*	1/4	0.05220(5)	0.3617(2)	0.0114(3)
Sn2	4*e*	1/4	0.58017(6)	0.0171(2)	0.0097(3)
Sn3	4*e*	1/4	0.64716(6)	0.3006(2)	0.0116(3)
Sn4	2*a*	1/4	1/4	0.0999(2)	0.0086(4)
Sn5	2*a*	1/4	1/4	0.4071(2)	0.0113(4)

Table 4
Atomic coordinates and isotropic displacement parameters for $Yb_3Cu_8Sn_4$

Atom	Position	*x*	*y*	*z*	*B* (Å^2)
Yb	6*c*	0.4764(1)	0.5236(1)	0[a]	0.74(5)
Cu1	6*c*	0.8362(6)	0.1638(6)	0.8440(9)	1.5(2)
Cu2	6*c*	0.8965(2)	0.1035(2)	0.5340(8)	0.42(9)
Cu3	2*b*	1/3	2/3	0.660(1)	0.7(3)
Cu4	2*a*	0	0	0.279(2)	0.5(2)
Sn1	6*c*	0.8299(3)	0.1701(3)	0.2123(7)	0.65(6)
Sn2	2*b*	1/3	2/3	0.2961(8)	1.4(2)

Space group $P6_3mc$ (No.186), $R_{wp} = 0.040$, $R_{exp} = 0.079$, $R_B = 0.069$.
[a] Arbitrarily fixed.

4. Discussion

Different from the other rare earths giving RCu$_2$Sn$_2$ phases (R = La–Nd, Sm [19,20], Gd, Lu, Y [21]) with $CaBe_2Ge_2$ structure, ytterbium shows two other compounds with close composition, $Yb_3Cu_6Sn_5$ isotypic with $Dy_3Co_6Sn_5$ [10] and $Yb_5Cu_{11}Sn_8$ with its own structure. Moreover, $Yb_5Cu_{11}Sn_8$ shows noticeable similarities with the structure of the phase $Ce_3Pd_6Sb_5$ [22], also having the same space group in common. All these compounds belong to the same family, originating from the $BaAl_4$ type and its ternary derivatives $ThCr_2Si_2$ and $CaBe_2Ge_2$. Extended reviews of the $BaAl_4$-derived structures were made by Parthé et al. [23] and more recently by Kussmann et al. [24].

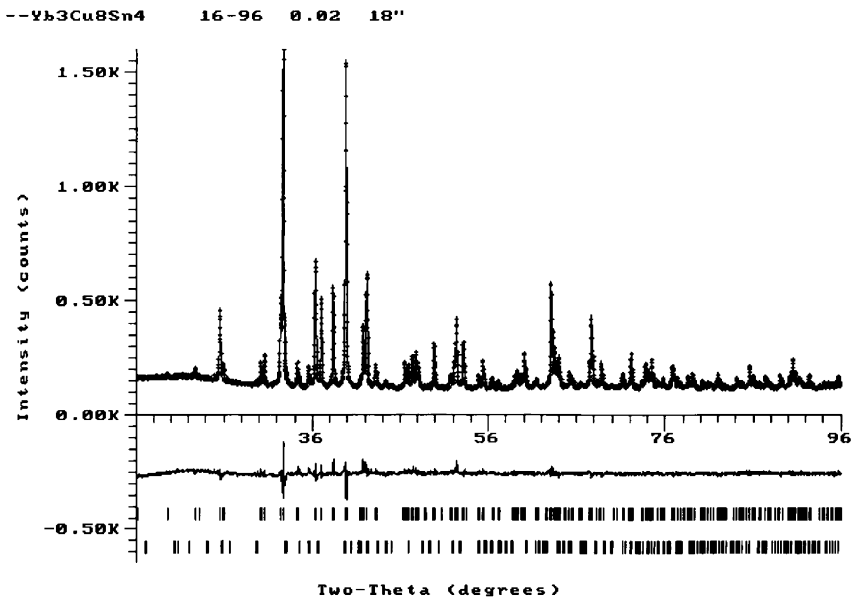

Fig. 1. Observed X-ray powder pattern (crosses) and Rietveld refinement profile (solid line) for the $Yb_3Cu_8Sn_4$ sample. The lower profile gives the difference between observed and calculated data; the Bragg angle positions are indicated by vertical bars for $Yb_3Cu_8Sn_4$ (upper row) and the Yb–Cu–Sn hexagonal phase related to $CeNi_5Sn$ (lower row).

Table 5
Interatomic distances (Å) for $Yb_3Cu_6Sn_5$ up to 16% greater than the sum of the metallic radii for CN12 [25]. The standard uncertainty is 0.001 Å for all distances

Yb1–2 Cu2	3.107	Yb2–4 Cu1	3.193
Yb1–4 Cu1	3.181	Yb2–8 Sn1	3.425
Yb1–4 Sn1	3.192	Yb2–4 Cu2	3.725
Yb1–2 Sn2	3.289	Yb2–2 Yb1	3.953
Yb1–2 Sn1	3.429	Yb2–2 Yb2	4.365
Yb1–2 Cu1	3.671		
Yb1–Yb2	3.953	Cu2–2 Sn1	2.650
Yb1–2 Yb1	4.365	Cu2–4 Cu1	2.693
		Cu2–2 Sn2	2.892
Cu1–2 Sn1	2.605	Cu2–2 Yb1	3.107
Cu1–Sn2	2.642	Cu2–2 Yb2	3.725
Cu1–2 Cu2	2.693		
Cu1–Sn1	2.754	Sn1–2 Cu1	2.605
Cu1–2 Yb1	3.181	Sn1–Cu2	2.650
Cu1–Yb2	3.193	Sn1–Cu1	2.754
Cu1–Yb1	3.671	Sn1–Sn1	3.001
		Sn1–2 Yb1	3.192
Sn2–4 Cu1	2.642	Sn1–2 Yb2	3.425
Sn2–4 Cu2	2.892	Sn1–Yb1	3.429
Sn2–4 Yb1	3.289	Sn1–2 Sn1	3.566

Fig. 2 shows the structural relationships among $Yb_5Cu_{11}Sn_8$, $Yb_3Cu_6Sn_5$ and $Ce_3Pd_6Sb_5$. Standardized atomic coordinates are used for the three compounds. The tetragonal $ThCr_2Si_2$ structure is adjoined for a comparison. The characteristic pseudo-body-centered subcell formed by the largest atoms is repeated five ($Yb_5Cu_{11}Sn_8$) and three times ($Yb_3Cu_6Sn_5$ and $Ce_3Pd_6Sb_5$). Owing to the strong distortion, $Yb_3Cu_6Sn_5$ shows a limited similarity with the parent $ThCr_2Si_2$, whereas $Yb_5Cu_{11}Sn_8$ and $Ce_3Pd_6Sb_5$ show practically half $ThCr_2Si_2$ cell reproduced five and three times, respectively, along their *b*-axis. These slabs, which cover approximately half cell, maintain the same composition as in the parent structure, being formed by a basket-shaped cluster of the (Cu,Sn) or (Pd,Sb) atoms sandwiched between two rare earth layers. In the other half cell, the composition of the cluster is defective and some distortion appears. The two clusters are joined by Pd–Sb bonds in $Ce_3Pd_6Sb_5$ as in the $CaBe_2Ge_2$ type (Be–Ge bonds), while in $Yb_5Cu_{11}Sn_8$ the connection is realized by both Cu–Sn and Sn–Sn bonds. For $Ce_3Pd_6Sb_5$ the Sb–Sb links in Fig. 2 involve a distance which is almost 11% greater than the sum of the elemental radii [25], and are only a guide for the eye.

The sequence of rare earth layers and partners clusters along *c* is Ce–Pd_2Sb_2–Ce–$Pd_2Sb_{1.33}$ in $Ce_3Pd_6Sb_5$ and Yb–Cu_2Sn_2–Yb–$Cu_{2.4}Sn_{1.2}$ in $Yb_5Cu_{11}Sn_8$. Both structures are defective in the Sb or Sn atoms, but the defective cluster of $Yb_5Cu_{11}Sn_8$ is richer in copper atoms. In $Yb_3Cu_6Sn_5$ ($Dy_3Co_6Sn_5$-type) both (Cu,Sn) clusters are crystallographically identical with composition $Cu_2Sn_{1.67}$, defective in Sn, and the similarity of the Yb2 surroundings with the parent $ThCr_2Si_2$ is evident in the central part of the drawing.

The regularity of the $ThCr_2Si_2$ slab in $Yb_5Cu_{11}Sn_8$ is also shown by the coordination of the component atoms, where analogous situations as in the parent structures are reproduced. Namely, the copper atoms (Cu3, Cu4, Cu6) are surrounded by a Sn tetrahedron interpenetrated with a Yb tetrahedron, with an environment very similar to that of the Cr atom in the $ThCr_2Si_2$

Table 6
Interatomic distances (Å) for $Yb_5Cu_{11}Sn_8$ up to 14% greater than the sum of the metallic radii for CN12 [25]

Yb1–Cu3	3.073(3)	Yb2–Cu4	3.052(3)
Yb1–2 Cu4	3.103(2)	Yb2–Cu5	3.092(3)
Yb1–Cu1	3.173(3)	Yb2–Cu6	3.184(4)
Yb1–2 Sn1	3.173(1)	Yb2–2 Cu3	3.191(2)
Yb1–2 Cu1	3.174(2)	Yb2–2 Sn5	3.264(1)
Yb1–Cu4	3.217(3)	Yb2–2 Sn1	3.290(1)
Yb1–2 Sn2	3.288(1)	Yb2–Sn2	3.339(2)
Yb1–2 Sn3	3.334(1)	Yb2–2 Cu2	3.340(3)
Yb1–Cu2	3.495(4)	Yb2–2 Sn4	3.556(1)
Yb1–Sn1	3.562(3)	Yb2–Sn3	3.814(2)
Yb1–Sn2	3.713(2)	Yb2–Yb2	4.280(2)
Yb1–Yb2	4.409(1)	Yb2–Yb1	4.409(1)
Yb1–2 Yb1	4.427(1)	Yb2–2 Yb2	4.427(1)
Yb3–2 Cu6	3.014(3)	Cu1–Cu2	2.516(4)
Yb3–Sn4	3.139(3)	Cu1–Sn2	2.599(3)
Yb3–2 Cu3	3.200(3)	Cu1–2 Sn2	2.643(2)
Yb3–4 Cu5	3.203(2)	Cu1–Sn1	2.646(4)
Yb3–4 Sn3	3.268(1)	Cu1–Yb1	3.173(3)
Yb3–Sn5	3.319(3)	Cu1–2 Yb1	3.174(2)
Yb3–2 Cu2	3.492(4)		
Yb3–2 Yb3	4.427(1)	Cu2–Cu1	2.516(4)
		Cu2–Sn4	2.591(3)
Cu3–Sn1	2.641(3)	Cu2–2 Cu5	2.596(2)
Cu3–Sn5	2.681(3)	Cu2–2 Sn2	2.624(2)
Cu3–2 Sn3	2.689(2)	Cu2–2 Yb2	3.340(3)
Cu3–Yb1	3.073(3)	Cu2–Yb3	3.492(4)
Cu3–2 Yb2	3.191(2)	Cu2–Yb1	3.495(4)
Cu3–Yb3	3.200(3)		
		Cu5–Cu5	2.450(5)
Cu4–2 Sn1	2.628(2)	Cu5–2 Cu2	2.596(2)
Cu4–Sn3	2.683(3)	Cu5–Sn2	2.624(3)
Cu4–Sn1	2.730(3)	Cu5–Sn3	2.787(3)
Cu4–Yb2	3.052(3)	Cu5–2 Sn4	2.789(2)
Cu4–2 Yb1	3.103(2)	Cu5–Yb2	3.092(3)
Cu4–Yb1	3.217(3)	Cu5–2 Yb3	3.203(2)
Cu6–2 Sn5	2.553(3)	Sn1–2 Cu4	2.628(2)
Cu6–2 Sn3	2.745(3)	Sn1–Cu3	2.641(3)
Cu6–2 Yb3	3.014(3)	Sn1–Cu1	2.646(4)
Cu6–2 Yb2	3.184(4)	Sn1–Cu4	2.730(3)
		Sn1–2 Yb1	3.173(1)
Sn2–Cu1	2.599(3)	Sn1–2 Yb2	3.290(1)
Sn2–2 Cu2	2.624(2)	Sn1–Yb1	3.562(3)
Sn2–Cu5	2.624(3)		
Sn2–2 Cu1	2.643(2)	Sn3–Cu4	2.683(3)
Sn2–Sn3	3.047(2)	Sn3–2 Cu3	2.689(2)
Sn2–2 Yb1	3.288(1)	Sn3–Cu6	2.745(3)
Sn2–Yb2	3.339(2)	Sn3–Cu5	2.787(3)
Sn2–Yb1	3.713(2)	Sn3–Sn2	3.047(2)
		Sn3–2 Yb3	3.268(1)
Sn4–2 Cu2	2.591(3)	Sn3–2 Yb1	3.334(1)
Sn4–4 Cu5	2.789(2)	Sn3–Yb2	3.814(2)
Sn4–Sn5	2.864(3)		
Sn4–Yb3	3.139(3)	Sn5–2 Cu6	2.553(3)
Sn4–4 Yb2	3.556(1)	Sn5–2 Cu3	2.681(3)
		Sn5–Sn4	2.864(3)
		Sn5–4 Yb2	3.264(1)
		Sn5–Yb3	3.319(3)

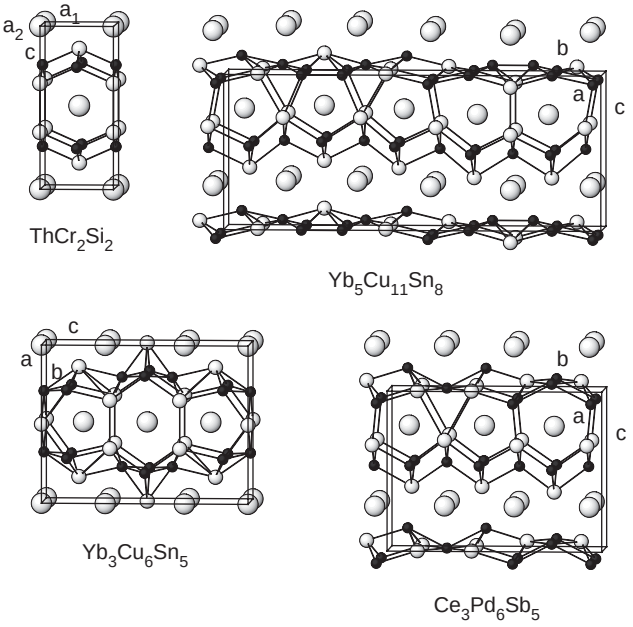

Fig. 2. Relationship among the orthorhombic $Yb_5Cu_{11}Sn_8$, $Yb_3Cu_6Sn_5$ ($Dy_3Co_6Sn_5$-type) and $Ce_3Pd_6Sb_5$ structures. The tetragonal $ThCr_2Si_2$ structure is adjoined for a comparison. Large circles: Th, Yb, Ce; medium circles: Si, Sn, Sb; small full circles: Cr, Cu, Pd.

type. On the other hand, Sn1, Sn3 and Sn5 occupy the center of square antiprisms formed by 4Cu and 4Yb with a square face capped by another Yb atom. The other square face is centered by a copper for Sn1 (as around a Ge atom in $CaBe_2Ge_2$), by a tin for Sn5 (as around silicon in $ThCr_2Si_2$), and by a copper plus a tin for Sn3. In most cases a pentagonal prism formed by copper and tin is found around the ytterbium atoms, capped on the faces by other atoms, generally at larger distances. The pentagonal prism around Yb1 in $Yb_3Cu_6Sn_5$ is identical to that of Yb3 in $Yb_4Cu_2Sn_5$ [8]. This coordination is very common in structures with two layers along a short axis, when all atoms lie on a mirror plane.

Two other members recently joined the large family of the $BaAl_4$-derived structures: $La_3Au_4In_7$ [26], a monoclinic distortion of the $Dy_3Co_6Sn_5$ type, with a different distribution of the (Au,In) atoms, leading to a defective structure in Au but richer in In atoms, and the orthorhombic $Ce_3Ni_7As_5$ [27], closely related to the $Ce_3Pd_6Sb_5$ structure.

The $Yb_3Cu_8Sn_4$ phase crystallizes with the ordered hexagonal structure already observed for the rare earth $R_3Co_8Sn_4$ compounds [16], $Eu_3Cu_8Sn_4$ [17] and $Ca_3Ni_8In_4$ [28]. This structure can be derived from the $BaLi_4$ type [29], by changing the space group from $P6_3/mmc$ to $P6_3mc$ and rearranging the atomic positions to obtain an ordered distribution of all atoms. Two of four Li positions in $P6_3/mmc$ are now split in $P6_3mc$,

and each couple of sites is occupied by copper and tin respectively, so that a distortion of the original $BaLi_4$ arrangement is achieved.

Compared with the sum of the elemental radii, the shortest distances in $Yb_3Cu_6Sn_5$ are Yb–Sn 3.192 Å (10% contraction), Cu–Sn 2.605 Å (10%), Sn–Sn 3.001 Å (8%) and Yb–Cu 3.107 Å (3%). Very similar values are found in $Yb_3Cu_8Sn_4$ with a further Cu–Cu contact at 2.49(1) Å (3%), but without Sn–Sn bonds. Interatomic distances in $Yb_5Cu_{11}Sn_8$ are somewhat more contracted and a minimum Cu–Cu distance is reached at 2.450 Å (4%). A comparison with analogous distances in the $CeCu_2Sn_2$ compound ($CaBe_2Ge_2$-type) [20] shows that a strong Cu–Sn bond occurs (2.48 Å), but no Cu–Cu contacts are formed.

In conclusion, the compound $Yb_3Cu_6Sn_5$ corresponds almost exactly to the τ_8 $Yb_{23}Cu_{42}Sn_{35}$ phase, already present in the Yb–Cu–Sn section. Two new compounds with similar Yb content and composition $Yb_5Cu_{11}Sn_8$ and $Yb_3Cu_8Sn_4$ were found. The crystal structure determination of phases occurring in the Cu-rich region of the Yb–Cu–Sn system is actually in course and will be the subject of another work.

References

[1] Y. Zhuang, C. Qin, J. Li, J. Less-Common Met. 175 (1991) 97–101.
[2] P. Riani, D. Mazzone, G. Zanicchi, R. Marazza, R. Ferro, F. Faudot, M. Harmelin, J. Phase Equilibria 19 (1998) 239–251.
[3] M.L. Fornasini, R. Marazza, D. Mazzone, P. Riani, G. Zanicchi, Z. Kristallogr. 213 (1998) 108–111.
[4] P. Riani, M.L. Fornasini, R. Marazza, D. Mazzone, G. Zanicchi, R. Ferro, Intermetallics 7 (1999) 835–846.
[5] G. Zanicchi, D. Mazzone, M.L. Fornasini, P. Riani, R. Marazza, R. Ferro, Intermetallics 7 (1999) 957–966.
[6] R. Ferro, P. Riani, G. Zanicchi, D. Mazzone, R. Marazza, G. Effenberg, J. Min. Metall. 35 (1999) 39–68.
[7] P. Riani, D. Mazzone, R. Marazza, G. Zanicchi, R. Ferro, Intermetallics 8 (2000) 259–266.
[8] M.L. Fornasini, G. Zanicchi, D. Mazzone, P. Riani, Z. Kristallogr. NCS 216 (2001) 21–22.
[9] K. Yvon, W. Jeitschko, E. Parthé, J. Appl. Crystallogr. 10 (1977) 73–74.
[10] R. Pöttgen, Z. Naturforsch. 50b (1995) 175–179.
[11] A.H. Gomes de Mesquita, K.H.J. Buschow, Acta Crystallogr. 22 (1967) 497–501.
[12] A. Altomare, M.C. Burla, M. Camalli, G.L. Cascarano, C. Giacovazzo, A. Guagliardi, A.G.G. Moliterni, G. Polidori, R. Spagna, J. Appl. Crystallogr. 32 (1999) 115–119.
[13] G.M. Sheldrick, SHELXL-97, Program for Refinement of Crystal Structures, University of Göttingen, Germany, 1997.
[14] L.M. Gelato, E. Parthé, J. Appl. Crystallogr. 20 (1987) 139–143.
[15] A. Mugnoli, A micro-computer program to survey empty spaces in a crystal structure, XIV European Crystallographic Meeting, Enschede (1992), Abstr. 530. Z. Kristallogr (Suppl.6).
[16] F. Canepa, S. Cirafici, M.L. Fornasini, P. Manfrinetti, F. Merlo, A. Palenzona, M. Pani, J. Alloys Compd. 297 (2000) 109–113.
[17] M.L. Fornasini, P. Manfrinetti, D. Mazzone, Z. Kristallogr. NCS 218 (2003) 279–280.
[18] R.A. Young, A. Sakthivel, T.S. Moss, C.O. Paiva-Santos, J. Appl. Crystallogr. 28 (1995) 366–367.
[19] R.V. Skolozdra, L.P. Komarovskaya, Ukr. Fiz. Zhur. 27 (1982) 1834–1838.
[20] E. Lidström, A.M. Ghandour, L. Häggström, Y. Andersson, J. Alloys Compd. 232 (1996) 95–100.
[21] K. Kaczmarska, J. Pierre, A. Slebarski, A. Starczewska, J. Magn. Magn. Mater. 127 (1993) 151–158.
[22] R.A. Gordon, F.J. DiSalvo, R. Pöttgen, J. Alloys Compd. 228 (1995) 16–22.
[23] E. Parthé, B. Chabot, H.F. Braun, N. Engel, Acta Crystallogr. B39 (1983) 588–595.
[24] D. Kussmann, R. Pöttgen, U.Ch. Rodewald, C. Rosenhahn, B.D. Mosel, G. Kotzyba, B. Künnen, Z. Naturforsch. 54b (1999) 1155–1164.
[25] E. Teatum, K.A. Gschneidner Jr., J. Waber, Rep. LA-4003, National Technical Information Service, Springfield, VA, USA, 1968.
[26] Y.V. Galadzhun, V.I. Zaremba, Y.M. Kalychak, R.-D. Hoffmann, R. Pöttgen, Z. Anorg. Allg. Chem. 626 (2000) 1773–1777.
[27] V. Babizhetskyy, R. Guérin, O. Isnard, K. Hiebl, J. Solid State Chem. 172 (2003) 265–276.
[28] V.I. Zaremba, I.R. Muts, Y.M. Kalychak, R.-D. Hoffmann, R. Pöttgen, J. Solid State Chem. 160 (2001) 415–420.
[29] F.E. Wang, F.A. Kanda, C.F. Miskell, A.J. King, Acta Crystallogr. 18 (1965) 24–31.